

# Effect of magnetic field on the laterally colliding plasma plumes

Alamgir Mondal, R. K. Singh, Vishnu Chaudhari, and H. C. Joshi  
*Institute for Plasma Research, HBNI, Bhat, Gandhinagar, Gujarat*  
 (Dated: July 28, 2022)

An experimental investigation of laser produced colliding plasma of aluminium target in the presence of external varying magnetic field is done under vacuum condition. Characteristic parameters and line emission of plasma plume in the presence of magnetic field are compared with those for field free case. Axial expansion of the plasma is slowed down in the presence of magnetic field as compared to the field free case. Contrary to the field free case no sharp interaction zone is observed. Higher electron temperature and increased ionic line emission from singly as well as doubly ionized aluminium can be attributed to the Joule heating phenomenon.

## I. INTRODUCTION

Collision of plasma plumes is an important phenomenon in many laboratory plasma and applications such as plasma confinement, inertial confinement fusion (ICF), laboratory studies of plasma of astrophysical importance, generation of nanoparticles and ion-sources etc.[1–6] Expansion of laser produced plasma in the presence of an external magnetic field has been studied experimentally under different conditions and has been illustrated in recent works.[1, 7–10] Colliding plasma with different targets, laser parameters, ambient and ablation geometries have been reported by several authors.[11–24] In our earlier work in aluminium colliding plasma we had found a clear distinct interaction zone and neutral emission is significantly enhanced at later times due to increase in three body recombination.[25]

Plasma-plasma interaction in the presence of external magnetic field is an interesting phenomenon to study because of its implications from the understanding fundamental physics as well as applications. Effect of magnetic field on the colliding plasma is quite interesting from the view point of its ramification in the plasmas of astrophysical importance to the technological aspect. To the the best of our knowledge, study regarding the colliding plasma in the presence of an external magnetic field has not been attempted so far. Therefore, in the present work we tried to explore the colliding plasma phenomenon in the presence of an external varying magnetic field by using fast imaging and optical emission spectroscopy(OES).

## II. EXPERIMENTAL SETUP

A schematic diagram of the experimental setup is shown in Fig. 1. A specially designed Helmholtz coil which can produce a transverse magnetic field varying from 0 to 6000 Gauss is placed inside a vacuum chamber. The coil has dimension of  $5 \times 5 \times 5 \text{ cm}^3$  and a flat-top magnetic profile which can be operated from outside without disturbing vacuum inside the chamber. Experiment is done in vacuum i.e.  $5 \times 10^{-7}$  mbar. Detailed experimental discussions on experimental setup are given elsewhere.[25] Briefly, laser beam of an Nd:YAG laser ( $\lambda = 1064 \text{ nm}$ , pulse width  $\sim 8 \text{ ns}$ , full-width at half-maximum) has been split into two beams of 100 mJ each. These two beams are focused by a plano-convex lens (35 cm

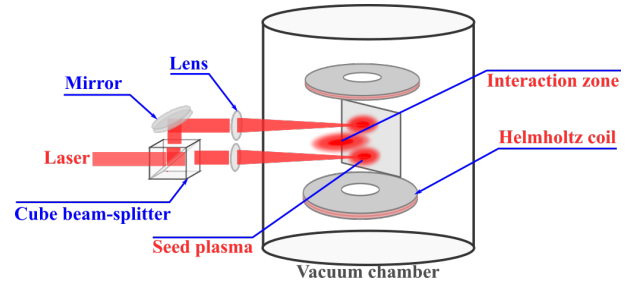


FIG. 1. Schematic diagram of the colliding plasma in presence of magnetic field.

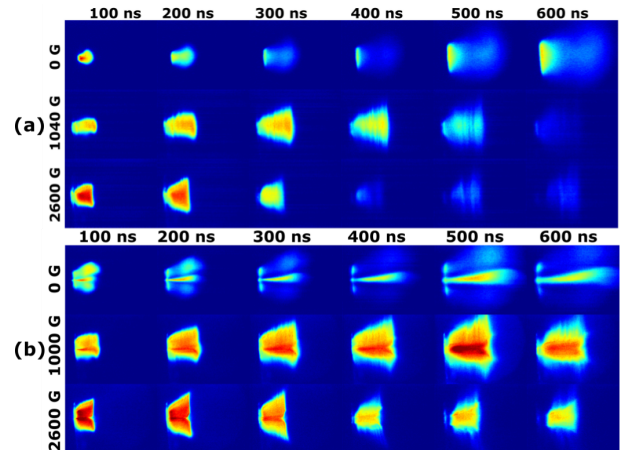


FIG. 2. Temporal evolution of (a) single plasma (b) colliding plasma with and without presence of constant external magnetic field.

focal length) on a clean aluminium target surface (99.9% purity). The target dimensions are  $6 \times 3 \times 1 \text{ cm}^3$  and is placed at the central region of the coil by using a vacuum compatible feed-through. The target positions are changed by 2 mm to a fresh surface after each consecutive 5 shots by using the linear scale on the feed-through. The experiment is done in single shot mode. The spot size and separation between the two beams are set as 1 mm and 4 mm, respectively. Magnetic field, ICCD camera, spectrograph and laser are synchronized with the combination of function generator and delay generator with jitter  $\sim 1 \text{ ns}$ .

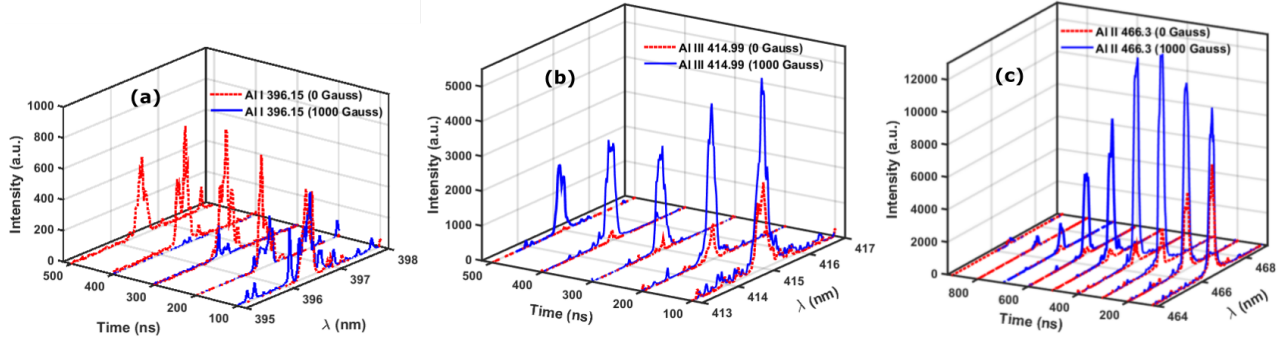


FIG. 3. Temporal evolution of (a) Al I 396.15, (b) Al III 414.9 and (c) Al II 466.3 nm with  $B = 0$  and 1000 Gauss from interaction zone.

### III. RESULTS AND DISCUSSION

#### A. Fast Imaging

Figure 2(a) shows temporal evolution of the laser produced single plasma plume in field free case and in the presence of magnetic field. All the images in this article are line integrated images in wavelength range of 350 to 700 nm and normalized to maximum intensity. The expansion of plasma without external field is free, adiabatic and its luminosity is beyond the detection limit at  $t > 1000$  ns. However, expansion dynamics and characteristics of the plasma changes with the introduction of transverse magnetic field. The major differences observed from this images are as follows. At shorter times i.e. from 100 to 300 ns the axial expansion velocity i.e. velocity perpendicular to the target surface, increases and then decreases at later time delays. This phenomenon can be attributed to plasma oscillations due to diamagnetic effect.[1, 26] After 300 ns free expansion of the plasma plume in axial direction appears to be slowed down by the resistive force induced by external magnetic field. On the other hand, plasma plume does not experience any resistive force along the field lines and therefore plume expand freely along the magnetic poles. A well resolved striation along the field lines is observed in presence of field, which is more pronounced at high field intensity and later stage of plasma. Striation phenomenon has been well studied by many authors in earlier works.[1, 27] Another important feature observed in presence of magnetic field is the increase of emission intensity of the plasma plume, where the luminosity of the plasma plume persists up to few microseconds. This is also supported by spectral data which will be discussed later.

To understand the behaviour of plasma dynamics in the presence of magnetic field, few parameters such as Larmor radii of electron and ion, plasma  $\beta$ , bubble radius ( $R_b$ ) and magnetic field diffusion time ( $t_d$ ) need to be estimated. Larmor radius is calculated from  $mv_{\perp}/qB$ , where  $m$ ,  $v_{\perp}$ ,  $q$  and  $B$  are mass of the charged particle, velocity perpendicular to the field, charge and magnetic field, respectively. Estimated values for electron,  $Al^+$  and  $Al^{2+}$  Larmor radii are  $3 \mu m$ ,  $7 cm$  and  $14 cm$ , respectively. In presence of magnetic field, plasma

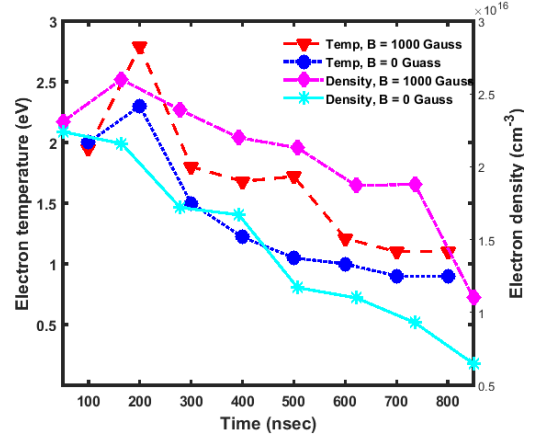


FIG. 4. Temporal evolution of electron temperature and density of colliding plasma with field  $B = 1000$  Gauss and without field. [will add better plot later]

$\beta$  governs the expansion dynamics of the plume. One of them is thermal beta which is the ratio of thermal pressure and magnetic pressure i.e.  $\beta_t = \frac{n_e T_e}{B^2/2\mu_0}$ , where all notations have their standard meanings. The expansion of the plasma plume transverse to the magnetic field will stop, when thermal beta will be equal to one i.e. thermal pressure of plasma will be equal to magnetic pressure. For the present experimental condition, the estimated value of thermal beta is around unity at 500 ns delay time. However, plasma plume does not stop at 500 ns rather it is slowed down as shown in Fig.2(a) and 2(b). This is because in laser produced plasma, thermal energy is converted into directed energy and hence thermal beta becomes important. The plasma expansion beyond the region  $\beta_t \approx 1$ , can be attributed to the directed beta  $\left(\beta_d = \frac{mn_e v^2/2}{B^2/2\mu_0}\right)$  of the plasma which is always greater than unity for the considered time delay.

Another important parameter is bubble radius which is de-

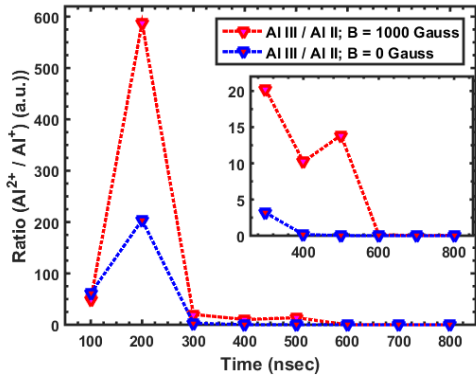


FIG. 5. Temporal evolution of  $\text{Al}^{2+}$  and  $\text{Al}^+$  ratio calculated from Saha equation with  $B = 1000$  Gauss and field free case.

scribed by  $R_b = \left( \frac{3\mu_o E_{lpp}}{2\pi B^2} \right)^{1/3}$  for a spherical plasma plume expanding in magnetic field. Where,  $\mu_o = 4\pi \times 10^7$  H/m,  $E_{lpp}$  is laser energy and  $B$  is the external magnetic field. The bubble radius, estimated from this equation is 1.77 cm for  $B = 1000$  Gauss, which is comparable to our plume dimension 2 cm as observed in images. The small difference observed in this case can be attributed to the assumption of spherical plasma plume, instead of elliptical nature of the plasma plume. Also magnetic diffusion time, described by  $t_d = \frac{4\pi\sigma R_b^2}{c^2}$ , where  $\sigma$  is plasma conductivity which can be estimated from Spitzer formula.[28] The estimated magnetic diffusion time for  $R_b = 1.77$  cm and 2 eV temperature is 537 ns for  $Z = 2$ . After this time magnetic field starts diffusing into the plasma plume. This fact is reflected in the spectroscopic observation on the line emission of  $\text{Al}^{2+}$  and  $\text{Al}^+$  discussed in the following section.

Figure 2(b) represents time integrated images of lateral interactions of two spatially separated plasma plumes in absence and presence of 1000 and 2600 Gauss magnetic field, respectively, for time delays 100 to 600 ns in vacuum. A well formed interaction zone is observed at the centre of interacting plumes which is moving with higher velocity in comparison to seed plumes, in absence of magnetic field. Interestingly the shape, size, geometry of the colliding plasma and the subsequent interaction zone exhibit drastic changes with the introduction of magnetic field. It can be seen from this figure that no clearly separated interaction zone is present in the presence of the field as observed in field free case. It seems like physical overlap between the transversally elongated plumes is there in presence of magnetic field. These changes can be understood as follows. The collisionality parameter  $\zeta = D/\lambda_{ii}$ , defined the nature of induced interaction zone, where,  $D$  is separation between two laser beams and  $\lambda_{ii} = [(m_i^2 v_{12}^2)/(4\pi e^4 Z^4 n_i \ln \Lambda_{12})]$ . [29] Here,  $m_i$ ,  $v_{12}$ ,  $Z$ ,  $n_i$  and  $\Lambda_{12}$  are the ion mass, relative velocity of two plumes, ionization level, plasma density and Coulomb logarithm of the plasma. The estimated collisionality parameters are  $\zeta = 5$  and

10 for  $B = 0$  and 1000 Gauss, respectively. These values predict soft stagnation for both the cases.

However, in presence of magnetic field, the ion-ion mean free path is modified because of ion gyration and hence affects the estimated parameters. In this scenario the collisionality parameter may not represent the true picture of interaction region in the presence of the field. This may be understood by the following facts. The Larmour radii for ions are bigger than the plume dimensions. Larger Larmour radii for the both  $\text{Al}^+$  and  $\text{Al}^{2+}$  as discussed earlier, may decrease the ion-ion collisions which causes the absence of clear interaction zone in magnetic field.

Further as in the case of single plasma plume, in colliding plasma also the expansion of the plasma plume in axial direction slows down in presence of field and the resistive force increases for higher field which can be seen by comparing images at  $B = 1000$  and 2600 Gauss. Visual examination of the Fig. 2(b) shows that optical emission from the plasma plume increases in the presence of field up to 400 ns delay time for both the fields (i.e. 1000 and 2600 Gauss) as compared to the field free case which can be attributed to increased ionic emission as will be discussed in the next section. In case of higher magnetic field, that is at 2600 G, the plasma luminosity decreases with further increase of time delay from 400 ns. This behaviour could be understood from the strong confinement of the plasma plume at later stage in higher magnetic field leading to the thermalization and hence decrease in emission intensity of the plasma plume. This is also confirmed by the spectral emission and electron temperature estimation as will be discussed latter. In order to see the effect of magnetic field on the lateral interaction of the plumes, the images of the colliding plasmas are recorded at different field values varying from 500-3200 G at delay time 400 ns as shown in Fig. 2(c). These images clearly demonstrate that dynamics and shape of the colliding plumes, overall luminosity and formation of interaction zone is highly dependent on the strength of magnetic field.

## B. Optical Emission Spectroscopy (OES)

Optical emission spectroscopy is used to investigate plasma electron temperature, density and variation in intensities of lines from various charge states. Figure 3 shows temporal changes in the intensity of characteristic Al I 396.15, Al II 466.3 and Al III 414.99 nm lines with  $B = 0$  and 1000 Gauss. Al I line shows increase in intensity at longer times for field free case. Interestingly its intensity is considerably diminished in the presence of the field (1000G) and almost unobservable at longer times which is in sharp contrast to field free case. On the other hand for ionic lines enhancement in intensity is observed. In contrast to the monotonic decrease in intensity in field free case [25], intensity of  $\text{Al}^+$  increases up to certain value at 300 ns delay time, as seen for Al II 466.3 nm, and then starts decreasing with further time delays. The enhancement in the intensity of  $\text{Al}^+$  ions is probably because of the increased temperature due to Joule heating in external field.[30] This is also supported by increase

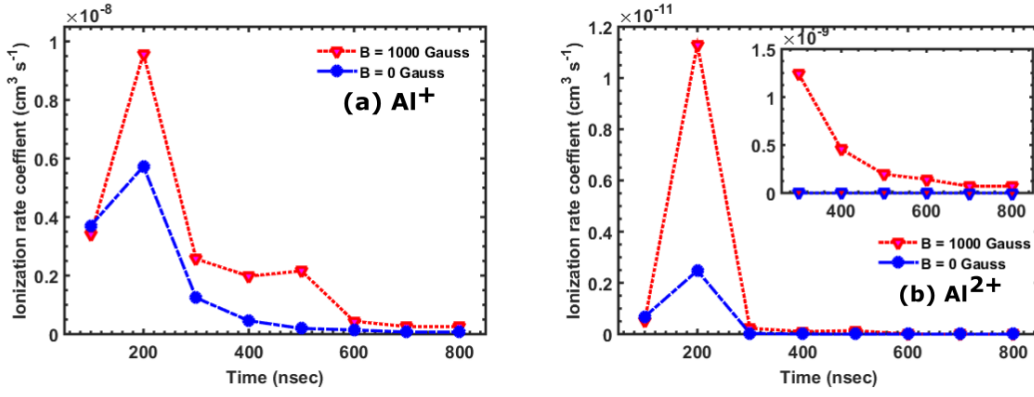


FIG. 6. Temporal evolution of ionization rate coefficient for (a)  $\text{Al}^+$  and (b)  $\text{Al}^{2+}$ .

in the ionization rate coefficients with introduction of magnetic field, which will be discussed latter. In the forgoing discussion, it is shown that the electron density is also increased after the introduction of magnetic field, which is in line with our observation regarding increased ionization. The intensity of Al II 466.3 nm line initially enhances with the increase of field strength up to 1000 Gauss and after that it decreases with further increase of field. Decrease in neutral line intensity and continuous increase in  $\text{Al}^{2+}$  intensity from  $B = 0$  Gauss is observed in the presence of magnetic field. As mentioned this can be attributed to the increase in plasma electron temperature and subsequent density because of Joule heating in the presence of magnetic field. Electron temperature has been estimated by using Boltzmann relation,  $I_{ij}/I_{kl} = [(v_{ij}A_{ij}g_i)/(v_{kl}A_{kl}g_k)] \exp[-(E_i - E_k)/(k_B T_e)]$ . [31] In this relation,  $I$  is the line intensity of the transition between two energy levels,  $v$  is the frequency of the line,  $A$  is Einstein's coefficient,  $g$  and  $E$  is statistical weight and energy of the particular energy level,  $k_B$  is Boltzmann constant,  $T_e$  is electron temperature, and the subscripts  $i, j, k$  and  $l$  denote different energy levels. Electron density is estimated by Al (II) line 466.3 nm as described in ref.[25].

Temporal evolutions of electron temperature and density of colliding plasma with and without  $B$  are shown in Fig. 4. It can be seen that electron temperature increases initially up to 200 ns time delay. After that it decreases with further delay time in field free case. The temporal profile of electron temperature in presence of magnetic field can be divided in three steps. After increasing at initial time, it decreases rapidly and is nearly unchanged within the range of 300 to 500 ns delay time. Again, it decreases from 500 to 600 ns. However, throughout this temporal evolution, the electron temperature is always higher in presence of magnetic field  $B$  as compared to field free case. Electron density is increased in the presence of magnetic but appears to show similar type of trend with time as in case of electron temperature.

Beside ionic line intensity, electron temperature and density, we have also calculated the ratio of  $\text{Al}^{2+}$  and  $\text{Al}^+$  and ionization rate coefficient. Ratio of  $\text{Al}^{2+}$  and  $\text{Al}^+$  ions  $\frac{n_i}{n_n}$  has been calculated by using Saha relation described by  $\frac{n_i}{n_n} \approx 2.4 \times 10^{21} \frac{T^{3/2}}{n_i} e^{U_i/k_B T}$  and is shown in Fig.5 for both the

cases i.e. with and without field.[32] Here,  $n_i, n_n, T, U_i, k_B$  represents ion density, neutral density, plasma temperature in Kelvin, ionization potential of atoms and Boltzmann constant, respectively. Figure 5 shows substantial increase in  $\text{Al}^{2+}$ . Ionization rate coefficient discussed in the next section also supports it.

Ionization rate coefficients for both  $\text{Al}^+$  and  $\text{Al}^{2+}$  lines with and without external field has been estimated from the eqn. 1.[33]

$$\kappa_{pi} = \frac{9.56 \times 10^{-6} (kT_e)^{-1.5} \exp(-\epsilon_{pi})}{\epsilon_{pi}^{2.33} + 4.38\epsilon_{pi} + 1.32\epsilon_{pi}} \text{ cm}^3 \text{ s}^{-1} \quad (1)$$

Here,  $\epsilon_{pi} = E_{pi}/kT_e$  and  $T_e, E_{pi}, p, i$  represents electron temperature, ionization potential, principal quantum numbers of initial and ground state, respectively. Figure 6 shows the temporal evolution of ionization rate coefficient of colliding plasma at  $B = 0$  and 1000 Gauss in vacuum. This figure shows an initial increase in ionization rate coefficient for both  $\text{Al}^+$  and  $\text{Al}^{2+}$  lines and then decreases with time. Further, it shows decrease from 200 to 300 ns delay time. After that, it decreases at slower rate with further delay time. However, the difference in this rate is clearly visible for both cases with the introduction of magnetic field which describe fairly the spectral behaviour of observed neutral and ionic lines (Fig. 3).

#### IV. CONCLUSION

It can be mentioned that the present study is an initiative in laser produced colliding plasma interaction in presence of an external magnetic field. Also an increase of  $\text{Al}^{2+}$  emission has been observed in the presence of the magnetic field as compared to field free case, which is attributed to Joule heating and subsequent increase in ionization. We believe the present work will be interesting from the view point of manipulating colliding plasma properties with the introduction of magnetic field.

- 
- [1] N. Behera, R. K. Singh, and A. Kumar, *Physics Letters A* **379**, 2215 (2015).
- [2] H. Iftikhar, S. Bashir, A. Dawood, M. Akram, A. Hayat, K. Mahmood, A. Zaheer, S. Amin, and F. Murtaza, *Laser and Particle Beams* **35**, 159 (2017).
- [3] Y. Li, C. Hu, H. Zhang, Z. Jiang, and Z. Li, *Applied optics* **48**, B105 (2009).
- [4] W. Gekelman, M. Van Zeeland, S. Vincena, and P. Pribyl, *Journal of Geophysical Research: Space Physics* **108** (2003).
- [5] B. H. Ripin, E. A. McLean, C. K. Manka, C. Pawley, J. A. Stamper, T. A. Peyser, A. N. Mostovych, J. Grun, A. B. Hassam, and J. Huba, *Physical review letters* **59**, 2299 (1987).
- [6] A. N. Mostovych, B. H. Ripin, and J. A. Stamper, *Physical review letters* **62**, 2837 (1989).
- [7] L. Dirnberger, P. Dyer, S. Farrar, and P. Key, *Applied Physics A* **59**, 311 (1994).
- [8] S. S. Harilal, B. O'shay, Y. Tao, and M. S. Tillack, *Applied Physics B* **86**, 547 (2007).
- [9] K. S. Singh, A. Khare, and A. K. Sharma, *Laser and Particle Beams* **35**, 352 (2017).
- [10] A. Dawood, S. Bashir, N. A. Chishti, M. A. Khan, and A. Hayat, *Laser and Particle Beams* **36**, 261 (2018).
- [11] A. De Giacomo, M. Dell'Aglio, A. Santagata, and R. Teghil, *Spectrochimica Acta Part B: Atomic Spectroscopy* **60**, 935 (2005).
- [12] B. Kumar, R. K. Singh, and A. Kumar, *Physics of Plasmas* **20**, 083511 (2013).
- [13] S. S. Harilal, C. V. Bindhu, V. P. Shevelko, and H. J. Kunze, *Laser and Particle Beams* **19**, 99 (2001).
- [14] S. L. Gupta, P. K. Pandey, and R. K. Thareja, *Physics of Plasmas* **20**, 013511 (2013).
- [15] E. Camps, L. Escobar-Alarcón, E. Haro-Poniatowski, and M. Fernández-Guasti, *Applied surface science* **197**, 239 (2002).
- [16] C. Sánchez Aké, R. Sanginés de Castro, H. Sobral, and M. Villagrán-Muniz, *Journal of applied physics* **100**, 053305 (2006).
- [17] P. Hough, C. McLoughlin, S. S. Harilal, J.-P. Mosnier, and J. T. Costello, *Journal of Applied Physics* **107**, 024904 (2010).
- [18] X. Li, Z. Yang, J. Wu, J. Han, W. Wei, S. Jia, and A. Qiu, *Journal of Applied Physics* **119**, 133301 (2016).
- [19] J. Dardis and J. T. Costello, *Spectrochimica Acta Part B: Atomic Spectroscopy* **65**, 627 (2010).
- [20] R. Sanginés, C. S. Aké, H. Sobral, and M. Villagrán-Muniz, *Physics Letters A* **367**, 351 (2007).
- [21] K. F. Al-Shboul, S. S. Harilal, S. M. Hassan, A. Hassanein, J. T. Costello, T. Yabuuchi, K. A. Tanaka, and Y. Hirooka, *Physics of Plasmas* **21**, 013502 (2014).
- [22] B. Kumar, R. K. Singh, S. Sengupta, P. K. Kaw, and A. Kumar, *Physics of Plasmas* **21**, 083510 (2014).
- [23] B. Kumar, R. K. Singh, S. Sengupta, P. K. Kaw, and A. Kumar, *Physics of Plasmas* **22**, 063505 (2015).
- [24] B. Kumar, R. K. Singh, and A. Kumar, *Physics of Plasmas* **23**, 043517 (2016).
- [25] A. Mondal, B. Kumar, R. Singh, H. Joshi, and A. Kumar, *Physics of Plasmas* **26**, 022102 (2019).
- [26] D. K. Bhadra, *The Physics of Fluids* **11**, 234 (1968).
- [27] N. Behera, R. K. Singh, V. Chaudhari, and A. Kumar, *Physics of Plasmas* **24**, 033511 (2017).
- [28] D. Book and J. D. Huba, *NRL plasma formulary*, Tech. Rep. (Naval Research Lab Washington DC Plasma Physics Div., 2002).
- [29] C. Chenais-Popovics, P. Renaudin, O. Rancu, F. Gilleron, J.-C. Gauthier, O. Larroche, O. Peyrusse, M. Dirksmöller, P. Sondhauss, T. Missalla, *et al.*, *Physics of Plasmas* **4**, 190 (1997).
- [30] S. S. Harilal, M. S. Tillack, B. O'shay, C. V. Bindhu, and F. Najmabadi, *Physical Review E* **69**, 026413 (2004).
- [31] S. Mukasa, S. Nomura, H. Toyota, T. Maehara, F. Abe, and A. Kawashima, *Journal of Applied Physics* **106**, 113302 (2009).
- [32] F. F. Chen, *Introduction to Plasma Physics and controlled fusion* (Plenum Press, New York and London, 1974).
- [33] L. Vriens and A. H. M. Smeets, *Physical Review A* **22**, 940 (1980).